

SyLMAND: a microfabrication beamline with wide spectral and beam power tuning range at the Canadian Light Source

Garth Wells,^a Sven Achenbach,^{b*} Venkat Subramanian,^a Michael Jacobs,^{a,b} David Klymyshyn,^b Swathi Iyer,^b Banafsheh Moazed,^b Jack Hanson,^b Chen Shen^b and Darcy Haluzan^b

Received 3 September 2018

Accepted 14 December 2018

Edited by Y. Amemiya, University of Tokyo, Japan

Keywords: X-ray lithography; beamlines; microfabrication; MEMS.

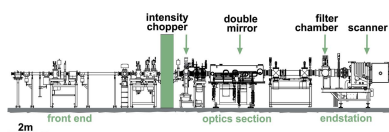
^aSynchrotron Laboratory for Micro and Nano Devices (SyLMAND), Canadian Light Source Inc., 44 Innovation Boulevard, Saskatoon, Saskatchewan S7N 2V3, Canada, and ^bElectrical and Computer Engineering, University of Saskatchewan, 57 Campus Drive, Saskatoon, Saskatchewan S7N 5A9, Canada. *Correspondence e-mail: s.achenbach@usask.ca

SyLMAND, the Synchrotron Laboratory for Micro and Nano Devices, is a recently commissioned microfabrication bend magnet beamline with ancillary cleanroom facilities at the Canadian Light Source. The synchrotron radiation is applied to pattern high-aspect-ratio polymer microstructures used in the area of micro-electro-mechanical systems (MEMS). SyLMAND particularly focuses on spectral and beam power adjustability and large exposable area formats in an inert gas atmosphere; a rotating-disk intensity chopper allows for independent beam-power reduction, while continuous spectral tuning between 1–2 keV and >15 keV photon energies is achieved using a double-mirror system and low-atomic-number filters. Homogeneous exposure of samples up to six inches in diameter is performed in the experimental endstation, a vertically scanning precision stage (scanner) with tilt and rotation capabilities under 100 mbar helium. Commissioning was completed in late 2017, and SyLMAND is currently ramping up its user program, mostly in the areas of RF MEMS, micro-fluidics/life sciences and micro-optics.

1. Introduction

High-aspect-ratio microstructures, *i.e.* with a large ratio of structure height to minimum lateral feature size, and with outstanding structure quality, can be fabricated by deep X-ray lithography (XRL) and optional subsequent process steps within the LIGA process (German acronym for lithography, electroplating and replication) (Becker *et al.*, 1986). In XRL, synchrotron radiation from an electron storage ring is applied to expose and thereby locally chemically modify a polymer resist. Several dedicated XRL beamlines and supporting laboratories across the world feature a wide range of beam properties (*e.g.* radiation spectrum, beam power, beam size), have various degrees of adjustability to process parameters, support a wide range of mask and sample types and geometries, and comprise different fabrication support ancillary facilities (Pantenburg & Mohr, 2001; Mohr *et al.*, 2004; Loechel *et al.*, 2002; Feiertag *et al.*, 1997; Guckel *et al.*, 1995; Johnson *et al.*, 1996; Aigeldinger *et al.*, 2000; Mancini *et al.*, 2002; Morales, 1999; Megtert *et al.*, 2007; Jian *et al.*, 2007; Utsumi *et al.*, 2007; Namkung, 1998; Chou *et al.*, 2008).

Adjustment of beam properties is key to achieving outstanding structure quality in high-aspect-ratio polymer structures: thicker resist layers require harder spectra (Mohr *et al.*, 1988). The reduction of secondary effects related to mask absorber thickness, mask membrane material and substrate



material, however, mandates the spectra to be as soft as possible for each exposure (Pantenburg & Mohr, 1995). Furthermore, the synchrotron beam power is responsible for temperature increases and associated thermal distortions in the mask and resist during exposure (Achenbach *et al.*, 2003).

Based on such previous research, SyLMAND was designed, built and recently commissioned to allow for optimized patterning with wide-ranging flexibility regarding the resist thickness as well as mask and substrate materials. The laboratory consists of a dedicated X-ray lithography beamline and supporting wet chemical and metrology laboratories in a single cleanroom environment. The focus of SyLMAND is on exposure conditions, particularly focusing on independent spectral and beam power adjustability, as well as a wide exposure fan for the processing of large samples under inert gas conditions.

2. Beamline design

2.1. Beamline overview

The SyLMAND beamline originates in bend magnet port 05B2-1 of the third-generation electron storage ring Canadian Light Source (CLS) in Saskatoon, Canada. The CLS is operated at an electron energy of 2.9 GeV and a maximum electron current of 220 mA. The critical photon energy is approximately 7.6 keV. Key performance parameters of the 16.91 m-long beamline include continuous spectral tuning between photon energies of 1–2 keV and >15 keV, independent beam-power adjustability and full six-inch wafer exposure capabilities under a 100 mbar helium atmosphere (Achenbach *et al.*, 2005, 2009). The major beamline components include an intensity chopper for power adjustment, a grazing-incidence double mirror system and a separate filter chamber for spectral adjustment of the ‘pink beam’, and the scanner endstation. Fig. 1 is an elevation drawing of the beamline with its key components from source point (not shown) to endstation. The illustration also shows that the optics and experimental sections are combined for better access and simplified cleanroom controls. The respective machine and beamline parameters are listed in Table 1.

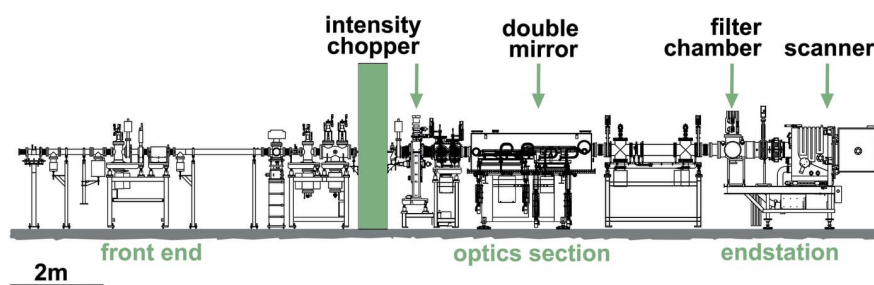


Figure 1

Elevation drawing of the SyLMAND beamline. By convention, the synchrotron beam propagates from the left (bend magnet source point, not shown) via the front end, through the concrete ratchet wall, into the combined optics and experimental sections inside a lead radiation protection and cleanroom-controlled hutch (hutch not shown).

Table 1

CLS machine parameters and SyLMAND beamline parameters.

Parameter	Present value
CLS electron beam	
Beam energy	2.9 GeV
Peak current	220 mA
Bend radius	7.143 m
SyLMAND beamline	
Source type	Bend magnet
Beamline length	16.91 m
Vacuum windows	110 μm Be
Intensity chopper	516 mm-diameter invar wheel rotating at 400 rpm, 100%, 25% or 10% open duty cycle, radiatively cooled
Double-mirror system	900 mm-long, Cr-coated Si bodies, water-cooled, 1st: bounce-up; 2nd: bounce-down; 4–45 mrad grazing-incidence angles (72 mm maximum vertical offset)
Scanner endstation	Scan velocity of 1–50 mm s ⁻¹ (or stationary), 100 mbar He atmosphere, filter chamber for low-energy cut-off, tilt module (0–60°) and rotation module (–180° to 180°); maximum format: 6 inch diameter (mask); 8 inch diameter (substrate)
Energy range	1–2 keV to >15 keV
Peak beam power	230 W (pink beam, without mirrors, at 220 mA)
Beam size, uncollimated	150 mm \times 8 mm

2.2. Beamline components

2.2.1. Intensity chopper. The overall beam power after the beryllium vacuum windows [10 μm downstream of the mirror system and 100 μm inside the scanner endstation with net dimensions of 150 mm (width) and 85 mm (height)] amounts to 230 W at an electron current of 220 mA. The majority of that power is not used for chemical modifications of the resist, but is dissipated as heat. This leads to a complicated temperature distribution which varies with time and location as the mask and sample are scanned through the beam and cooled to 25°C on the sides and back. Local temperature rises result in associated thermal expansion, causing thermal distortions during exposure, which ultimately reduce the microstructure accuracy (Achenbach *et al.*, 2003). SyLMAND provides the capability to reduce the incident beam power to limit thermal distortions to a level deemed acceptable for the individual patterning task, usually determined by micro-device performance requirements. This independent beam-power adjustment is achieved using a rotating disk chopper. The chopper temporarily blocks the propagation of the beam and therefore time-modulates the incoming radiation, reducing the average transmitted beam intensity based on the duty cycle of open/opaque disk areas. The duty cycle can be set to 100% (completely open; chopper retracted), 25% or 10% open duty cycle (only 10% of the photons transmitted) without affecting the spectral distribution.

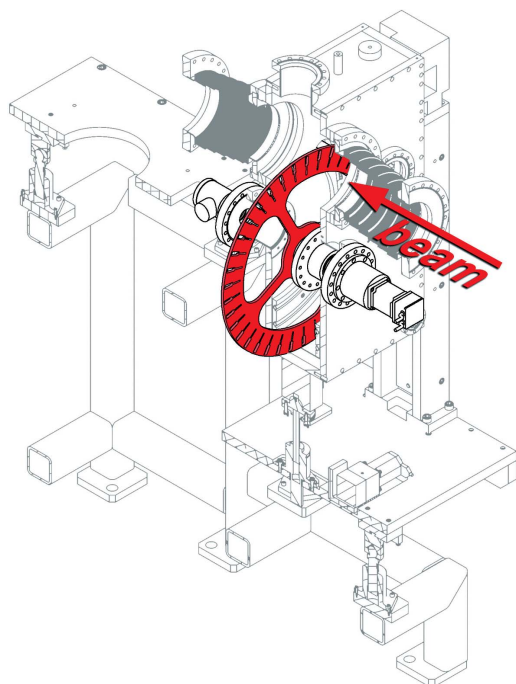


Figure 2
Drawing of the intensity chopper with highlighted disk (solid red color, 51.6 cm diameter, 38 openings) and synchrotron beam position.

The chopper consists of a massive invar-36 wheel roughly 52 cm in diameter with 38 openings, mounted orthogonally to the direction of the beam (see Fig. 2). When inserted into the beam, the disk can be moved to different vertical positions for the selection between pre-set widths of the individual openings (*i.e.* different duty cycles). This vertical adjustment is achieved by an external motor lifting the complete chopper system and is based on deformable bellows connecting to the stationary beamline on either side of the chopper. Driven by a magnetically coupled external motor, the disk rotates at typically 400 rpm. When intercepting the beam, the opaque chopper areas block the beam for up to 2 ms at any given location. During this time, the sample is vertically moved in the scanner by no more than 40 μm . This movement is insignificant compared with the beam height of several millimetres, ensuring homogeneous exposure of the sample. The chopper is located in a vacuum environment and is radiatively cooled. The maximum steady-state temperature at an emissivity of stainless steel of $\varepsilon = 0.57$ (worst-case assumption) has been simulated to be 350°C (Nagarkal *et al.*, 2008). Due to an increased emissivity of the roughened surface, actual temperatures at different load values were measured by infrared-remote thermal sensing to be between 130°C and 200°C.

Future upgrades with a co-rotating second disk with adjustable phase relative to the first disk will allow for a continuous power adjustment between 50% and 0% open duty cycle (Achenbach *et al.*, 2005).

The chopper will be increasingly required, as a top-up injection mode at constant electron current becomes implemented at the CLS: this machine mode will lead to a higher

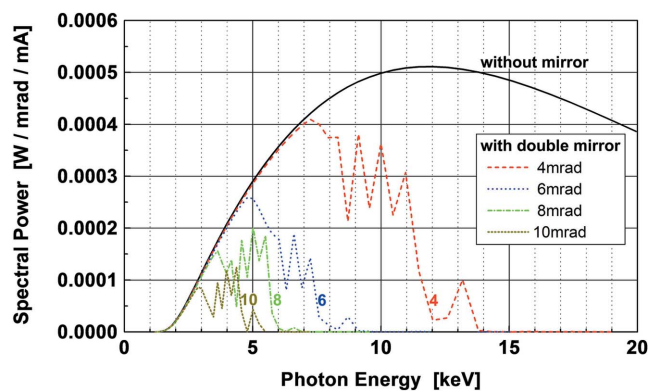


Figure 3
Simulated spectral power after 110 μm beryllium vacuum windows, without the mirror system and with the double mirror system at various grazing-incidence angles between 4 mrad and 10 mrad, for Cr mirror surfaces, oxidized 25 nm deep and coated with 100 nm carbon, and for a common layer roughness of 0.5 nm.

average constant beam power. All beamline components therefore remain at a constant temperature, which reduces the long-term drift of thermal conditions during an exposure of several hours. The combination of chopper and top-up mode therefore allows us to minimize thermal deformations and keep the remaining thermal artifacts constant over time and reproducible from sample to sample.

2.2.2. Double-mirror system. At SyLMAND, the spectral power after passing the two beryllium vacuum windows has its maximum intensity around 11 keV as depicted in the curve labeled ‘without mirror’ in Fig. 3. Most lithographic applications, however, require a pink beam with a softer spectrum. At SyLMAND, this spectral adjustment is achieved by high-energy cut-off using a flat, chromium-coated double-mirror system with grazing-incidence angles of 4 mrad to 45 mrad. The double-mirror system can be moved into the beam when needed; it consists of two water-cooled, flat silicon mirrors coated with 120 nm of chromium. The absorption edge of the chromium coating at 5.99 keV supports the suppression of higher energies as desired in many XRL patterning tasks. Assuming that the top 25 nm of the chromium are oxidized, the presence of a carbon contamination top layer of about 100 nm, and 0.5 nm roughness of all involved layers (Achenbach, Wells & Shen, 2018), simulated spectra for selected mirror angles are illustrated in Fig. 3. At 4 mrad, for instance, the cut-off energy is around $\varepsilon_{\text{cut-off}} \simeq 11.5$ keV, while, at 10 mrad, the cut-off energy has decreased to $\varepsilon_{\text{cut-off}} \simeq 4.5$ keV.

The double-mirror system with a first, upward deflecting and a second, downward deflecting mirror allows for adjustment of the mirror angles to each patterning task without realignment of the beamline. At 900 mm net mirror length and 800 mm mirror pole separation, the vertical beam offset varies from 6.4 mm for 4 mrad to 72 mm for 45 mrad.

The double-mirror system is equipped with eight fly wire and blade beam position and intensity monitoring systems for *in situ* diagnostics of beam position and beam properties before and after each mirror (Subramanian *et al.*, 2009). Fig. 4 illustrates the mirror system with the mirror bodies highlighted in solid red.

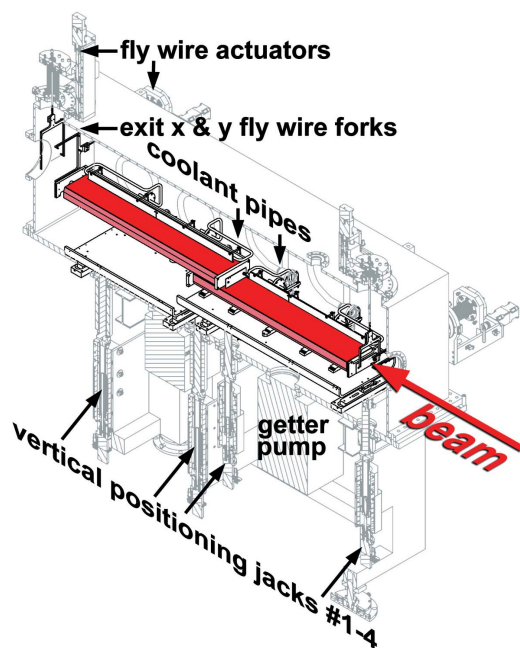


Figure 4
Drawing of the double-mirror system with highlighted mirror bodies (solid red color, 90 cm length, 80 cm offset) and synchrotron beam position.

Besides the mirror system, additional spectral tuning to achieve low-energy cut-off can be performed by inserting low-atomic-number filters, predominantly carbon sheets of thicknesses between 75 μm and 1250 μm . These filters are located in a dedicated filter chamber in the X-ray scanner (compare Fig. 1).

2.2.3. X-ray scanner endstation. At the sample, the synchrotron beam is approximately 160 mm wide and a maximum of 8 mm high. For homogeneous exposure of larger samples, the substrate and X-ray mask are mounted onto a cooled stage that is vertically oscillated through the beam in a scanner endstation. The SyLMAND vacuum scanner is an enhanced and larger version of commercial Jenoptik scanners installed at KARA (former ANKA), BESSY and CAMD storage rings. Full six-inch wafers can be exposed, and substrates up to eight inches can be mounted. Tilt and rotation capabilities of the stage allow for inclined exposures relative to the incident beam, enabling the fabrication of quasi-3D polymer microstructures. Exposures are typically carried out at 100 mbar He pressure in the working chamber to minimize photon absorption and to maximize conductive cooling of the substrate and mask. A beryllium vacuum window and a load lock system with the final gate valve separate the beamline high vacuum from the scanner rough vacuum and from ambient air. A filter chamber houses low-energy cut-off filters. Fig. 5 shows a drawing of the scanner with its key components and the scanning stage highlighted in solid red, while Fig. 6 is a photograph showing the user access to the scanner with its opened access door at the back end of the beamline. The scanner is programmed with the respective sample parameters to control the beamline for automated exposure once the chopper and mirror parameters have been set.

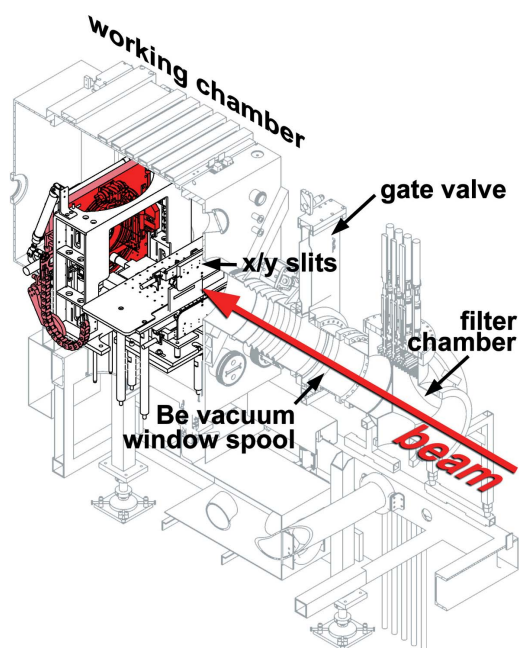


Figure 5
Drawing of the scanner endstation with highlighted vertical scanning stage (solid red color, holds samples up to eight inches in diameter and masks with up to six-inch exposable diameters) inside the vacuum working chamber, and synchrotron beam position.

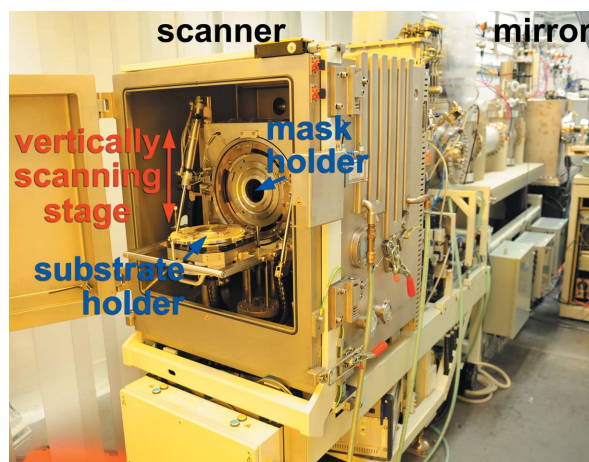


Figure 6
Photograph of the scanner endstation with opened access door, showing the vertical scanning stage with the mask and substrate holders.

2.2.4. Beam collimation and vacuum isolation. Further beamline components not explicitly mentioned before, and depicted but not highlighted in Fig. 1, include two sets of vertically and horizontally collimating slits. One set is located immediately upstream of the mirrors and the second is immediately upstream from the sample in the scanner.

Vacuum separation between the ultra-high vacuum in the storage ring and the rough vacuum in the scanner is achieved by two beryllium vacuum windows. The horizontal beam fan width of 150 mm to 160 mm, and the vertical beam offset in the double-mirror system of up to 72 mm when spectrally adjusting the beam, require a net exposable window area of 150 mm (width) by 85 mm (height). The combined window

thickness is minimized to 110 μm to reduce unwanted absorption of low-energy photons between 1 keV and 2 keV, particularly during soft X-ray exposure (Achenbach *et al.*, 2009). The mechanical stability for such large, but thin, windows is maintained by minimizing the maximum differential pressure across both windows; the first window is located in the spool piece downstream from the mirror. It is 10 μm thick and does not need to withstand significant pressure differences. It is not vacuum tight, but is bypassed with a thin vacuum tube. The window is designed to only reduce the conductance along the beamline, enabling differential pumping in an otherwise large-cross-section vacuum spool. The second window is a 100 μm -thick vacuum-tight window located inside the scanner; it can safely withstand 300 mbar differential pressure (Achenbach *et al.*, 2008). During exposures at 100 mbar helium, such a window can therefore safely be applied. A load lock system inside the scanner separates this vacuum from ambient pressure when the samples and masks are being mounted.

2.3. Ancillary facilities: sample pre- and post-processing cleanroom

Microfabrication at the SyLMAND beamline depends on the supporting integral cleanroom environment for sample pre- and post-processing, inspection and analysis. Thin-film metal deposition by magnetron sputtering and thick resist layer application by gluing, dry-film lamination or spin coating are core pre-processing capabilities. Further basic infrastructure enables sample processing by reactive ion etching and thermal treatment. Besides standard resist development, post-processing most importantly comprises high-aspect-ratio gold and nickel electroplating. Optical and electron microscopy as well as white-light interferometry are in-house inspection capabilities at SyLMAND.

3. X-ray mask fabrication

X-ray masks are indispensable tools for every XRL exposure. At SyLMAND, a variety of externally fabricated XRL mask formats can be accommodated. Alternatively, a proprietary XRL mask fabrication process has recently been developed at SyLMAND, offering a complete microfabrication value chain from mask fabrication to XRL processing and electroplating: the beam-power tuning capabilities described earlier allow the use of low thermal expansion coefficient polymers as mask membranes by limiting thermal distortions (Achenbach *et al.*, 2018). The SyLMAND 355 nm UV-laser writer by Heidelberg Instruments is used for primary patterning of the XRL mask resist templates on the polymer membrane, followed by nickel and gold electroplating of the absorber structures (Achenbach, Wells, Jacobs *et al.*, 2018).

4. Facility access

Access to the CLS facilities and beamlines is granted on a merit-based scheme. Proposals are accepted in bi-annual calls

and are independently peer-reviewed. Projects at SyLMAND are valid for up to two years. Urgent microfabrication processing requirements can also be requested throughout the year through a rapid access protocol, with the expectation to be later transferred into regular peer-reviewed proposals. Besides the peer-reviewed scheme, industrial clients can also access SyLMAND with intellectual property protection by paying for services ranging from beam time only to full service processing.

5. Conclusions

The overall beamline concept, design aspects, and performance characteristics of SyLMAND at the CLS have been discussed. SyLMAND uses bend-magnet radiation for exposure of wafers up to six inches in diameter under vacuum. Rotated and tilted exposures can also be performed. Continuous spectral adjustment between 1–2 keV and >15 keV photon energies is achieved by a flat, chromium-coated double silicon mirror system with grazing incidence angles of 0 mrad and 4 mrad to 45 mrad for high-energy cut-off, and low-atomic-number filters for low-energy cut-off. A rotating disk intensity chopper with pre-set duty cycles time-modulates the incoming beam and reduces the average transmitted beam intensity. This unique, independent spectral and beam power adjustability at large exposure formats under vacuum conditions allows us to optimize the beam characteristics for each patterning task for improved microstructure quality. Pre- and post-processing capabilities in the SyLMAND cleanroom as well as a new X-ray mask fabrication process, based on polymer mask membranes, direct laser writing and electroplating, offer a complete XRL fabrication sequence. Since late 2017, SyLMAND is in regular user mode and is accepting user proposals on a merit-based access scheme.

Acknowledgements

Spectral and beam-power calculations have been performed in part by using the LEX-D simulation tool developed by Stewart K. Griffiths and colleagues at Sandia National Laboratories, Livermore, USA. The authors would like to thank all the staff at the CLS that were involved in the design, construction and commissioning of SyLMAND for their support and contributions. We are particularly grateful to Emil Hallin and Bill Thomlinson of the CLS and the Saskatoon staff of TR Labs for helping to kick off the SyLMAND project.

References

- Achenbach, S., Klymyshyn, D. & Subramanian, V. (2005). *Conceptual Design Report for SyLMAND 'Synchrotron Laboratory for Micro and Nano Devices'*. The Canadian Light Source Inc., Saskatoon, SK, Canada.
- Achenbach, S., Klymyshyn, D., Subramanian, V., Reuther, F., Mullin, C., Wells, G. & Nagarkal, V. (2008). *15th Pan-American Synchrotron Radiation Instrumentation Conference (SRI2008)*, 10–13 June 2008, Saskatoon, Canada. S-56.
- Achenbach, S., Pantenburg, F. J. & Mohr, J. (2003). *Microsyst. Technol.* **9**, 220–224.

- Achenbach, S., Shen, C. & Wells, G. (2018). *J. Vac. Sci. Technol. B*, **36**, 012001.
- Achenbach, S., Subramanian, V., Klymyshyn, D. & Wells, G. (2009). *Microsyst. Technol.* **16**, 1293–1298.
- Achenbach, S., Wells, G., Jacobs, M., Moazed, B., Iyer, S. & Hanson, J. (2018). *Rev. Sci. Instrum.* **89**, 115001.
- Achenbach, S., Wells, G. & Shen, C. (2018). *J. Synchrotron Rad.* **25**, 729–737.
- Aigeldinger, G., Coane, P., Craft, B., Goettert, J., Ledger, S., Ling, Z. G., Manohara, H. & Rupp, L. (2000). *Proc. SPIE*, **4019**, 429–435.
- Becker, E. W., Ehrfeld, W., Hagmann, P., Maner, A. & Münchmeyer, D. (1986). *Microelectron. Eng.* **4**, 36–56.
- Chou, M. C., Pan, C. T., Wu, T. T. & Wu, C. T. (2008). *Sens. Actuators A Phys.* **141**, 703–711.
- Feiertag, G., Ehrfeld, W., Lehr, H., Schmidt, A. & Schmidt, M. (1997). *J. Micromech. Microeng.* **7**, 323–331.
- Guckel, H., Christenson, T. R. & Skrobis, K. (1995). *Formation of Microstructures Using a Preformed Photoresist Sheet*. US Patent 5378583.
- Jian, L. K., Casse, B. D. F., Heussler, S. P., Kong, H. R., Moser, H. O., Ren, Y. P., Saw, B. T. & bin Mahmood, S. (2007). *AIP Conf. Proc.* **879**, 1512–1515.
- Johnson, E. D., Milne, J. C., Siddons, D. P., Guckel, H. & Klein, J. L. (1996). *Synchrotron Radiat News*, **9**(4), 10–13.
- Loechel, B., Jian, L., Scheunemann, H. U., Schondelmaier, D., Goettert, J. & Desta, Y. M. (2002). *Proceedings of the 7th International Commercialization of Micro and Nano Systems Conference (COMS 2002)*, 8–12 September 2002, Ypsilanti, MI, USA.
- Mancini, D., Moldovan, N., Divan, R., DeCarlo, F. & Yaeger, J. (2002). *Proc. SPIE*, **4783**, 28–36.
- Megttert, S., Bouamrane, F. & Bouvert, T. (2007). *Proceedings of the 7th International Workshop on High-Aspect-Ratio Micro-Structure Technology (HARMST 2007)*, June 2007, Besancon, France, pp. 27–28.
- Mohr, J., Achenbach, S., Börner, M. & Schulz, J. (2004). *Research Activities in the LIGA Laboratory at ANKA*, pp. 10–15. ANKA Beamline, Karlsruhe, Germany.
- Mohr, J., Ehrfeld, W. & Münchmeyer, D. (1988). *Analyse der Defektursachen und der Genauigkeit der Strukturübertragung bei der Röntgentiefenlithographie mit Synchrotronstrahlung*. Kernforschungszentrum Karlsruhe, Germany.
- Morales, A. (1999). Report 99-8228. Sandia National Laboratories, Livermore, USA.
- Nagarkal, V., Mullin, C., Achenbach, S., Subramanian, V. & Wells, G. (2008). *Proceedings of the 5th International Workshop on Mechanical Engineering Design of Synchrotron Radiation Equipment and Instrumentation (MEDSI)*, 10–13 June 2008, Saskatoon, Canada, p. 105.
- Namkung, W. (1998). *J. Synchrotron Rad.* **5**, 158–161.
- Pantenburg, F. J. & Mohr, J. (1995). *Nucl. Instrum. Methods Phys. Res. B*, **97**, 551–556.
- Pantenburg, F. J. & Mohr, J. (2001). *Nucl. Instrum. Methods Phys. Res. A*, **467–468**, 1269–1273.
- Subramanian, V., Achenbach, S., Klymyshyn, D., Wells, G., Dolton, W., Nagarkal, V., Mullin, C. & Augustin, M. (2009). *Microsyst. Technol.* **16**, 1547–1551.
- Utsumi, Y., Kishimoto, T., Hattori, T. & Hara, H. (2007). *Microsyst. Technol.* **13**, 417–423.